Ballistic hole magnetic microscopy

E. Haq, T. Banerjee, M. H. Siekman, J. C. Lodder, and R. Jansen[a)]
MESA+ Institute for Nanotechnology, University of Twente, 7500 AE Enschede, The Netherlands

(Received 18 October 2004; accepted 6 January 2005; published online 15 February 2005)

A technique to study nanoscale spin transport of holes is presented: ballistic hole magnetic microscopy. The tip of a scanning tunneling microscope is used to inject hot electrons into a ferromagnetic heterostructure, where inelastic decay creates a distribution of electron-hole pairs. Spin-dependent transmission of the excited hot holes into an underlying *p*-type semiconductor collector induces a hole current in the valence band of the semiconductor, with magnetocurrent values up to 180%. The spin-filtering of holes is used to obtain local hysteresis loops and magnetic imaging with spatial resolution better than 30 nm. © *2005 American Institute of Physics*. [DOI: 10.1063/1.1864243]

Introduced by Bell and Kaiser in 1988, ballistic electron emission microscopy (BEEM)[1] has proven to be a powerful technique to study the nanoscale properties of a wide variety of structures. These include buried metal-semiconductor interfaces, semiconductor heterostructures and quantum dots, ultrathin gate as well as tunnel oxides, and metallic and silicide thin films.[2–6] The high spatial resolution makes it an attractive technique for the study of magnetic nano- and heterostructures which form the basis of spintronics and magnetic data storage. The extension of BEEM to its spin-sensitive counterpart, ballistic electron magnetic microscopy, was demonstrated to allow magnetic imaging with nanoscale resolution.[7,8]

The high resolution and versatility of the technique stem from the use of the tip of a scanning tunneling microscope (STM) to inject nonequilibrium carriers into the structure under investigation, and collection of the transmitted carriers in a semiconductor. Mostly, the injected carriers are hot electrons and the collector is an *n*-type semiconductor. However, it has been shown[9,10] that the technique can equally well be applied using nonequilibrium holes, in combination with a *p*-type collector. With hole BEEM, dislocation lines have been resolved with 1.5 nm resolution.[11] Moreover, on Au/Si and Au/GaAs systems, BEEM in reverse (or scattering) mode was demonstrated,[10] where instead of the ballistically transmitted carriers, the carriers that are created in the inelastic scattering of the injected hot carriers are collected. However, in none of the hole-based or the reverse modes of BEEM has spin sensitivity been addressed.

In this work we introduce a spin-sensitive version of BEEM using holes: ballistic hole magnetic microscopy in reverse mode (R-BHMM). We demonstrate that this technique can be used to study local spin-dependent transport in ferromagnetic metal-semiconductor structures and allows magnetic imaging with nanoscale resolution. This hole-based technique can be applied to systems which require a *p*-type semiconductor, either for device operation or due to material aspects. Moreover, if holes can cross the Schottky barrier without losing spin information, the method may find an important application in spin injection of holes into a semiconductor, complementary to spin injection of electrons into the conduction band of *n*-type semiconductors.[12,13]

The principle of the technique is illustrated in Fig. 1. The sample consists of a *p*-type semiconductor substrate coated with a metal thin film stack containing two ferromagnetic layers. Although the STM tip can be used to inject hot holes directly into the metal stack, we found[14] that the transmitted current is rather small, making imaging more challenging. However, the signal is improved significantly when the tip voltage is kept negative, such that hot electrons are injected. In this reverse mode, the injected hot electrons decay inelastically via electron-hole (e-h) pair excitation. The hot holes thus created can be transmitted through the metal stack and enter the valence band of the underlying *p*-type semiconductor, provided the holes have retained sufficient energy and the proper momentum to overcome the Schottky barrier at the metal/semiconductor interface. If the holes, once created, have spin-dependent attenuation lengths in the ferromagnetic layers, the collected hole current will depend on the relative magnetization alignment of the two ferromagnets. Note that hot-electron decay lengths in ferromagnets are much shorter[15] than in normal metals like Au, such that holes created in the nonmagnetic spacer layers can be neglected.

The samples were deposited by thermal evaporation in a molecular beam epitaxy system with a base pressure of 10^{-10} mbar. Substrates consist of HF-etched *p*-Si(100) with a

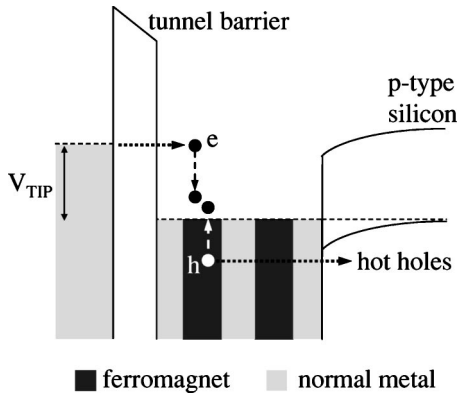

FIG. 1. Schematic energy diagram of ballistic hole magnetic microscopy in reverse mode. Hot electrons are injected from a STM tip into a magnetic multilayer stack on a *p*-type semiconductor collector. Inelastic scattering in the magnetic layers creates electron-hole (e-h) pairs, inducing a spin-dependent hole current into the valence band of the semiconductor.

a)Author to whom correspondence should be addressed; electronic mail: ron.jansen@ewi.utwente.nl

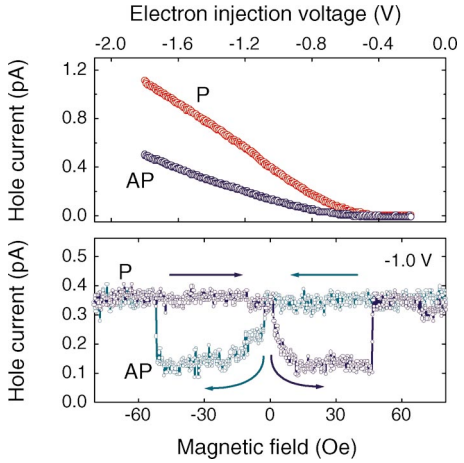

FIG. 2. (Color) (top panel) Hole current vs tip voltage for *p*-Si/Au(70 Å)/$Ni_{81}Fe_{19}$(18 Å)/Au(70 Å)/Co(18 Å)/Au(30 Å) at a magnetic field of +100 and −25 Oe, respectively, corresponding to parallel (*P*) and antiparallel (*AP*) alignment of the $Ni_{81}Fe_{19}$ and Co magnetization. Injection current is I_T=4 nA. (bottom panel) Hole current vs magnetic field at tip bias V_T=−1.0 V and injection current I_T=4 nA. All data at T=150 K.

lithographically defined area of 150 μm diameter, surrounded by a thick SiO_2 insulator. First, a 70 Å Au layer is grown to form a high quality Schottky barrier of 0.3±0.03 eV with a smooth surface onto which the rest of the metal layer stack is grown. Samples used here are $Ni_{81}Fe_{19}$/Au(70 Å)/Co spin valves where both magnetic layers are either 15 or 18 Å thick. A 30 Å Au cap layer is deposited in the end to provide a chemically inert surface for *ex situ* sample transfer. BHMM measurements are performed at 150 K in a modified variable temperature ultrahigh vacuum STM, with a base pressure of 10^{-10} mbar. Current coils provide a homogeneous in-plane magnetic field. For all measurements, the metal surface is grounded and negative voltage (V_T) is applied to the PtIr tip with the tunnel current I_T kept constant using feedback. A contact to the back of the *p*-type Si is used to detect the hole current I_{hole} with a two-stage amplifier (10^{11} V/A) and a 300 Hz low-pass filter. More details are described elsewhere.[16]

Representative hole spectra are shown in the top panel of Fig. 2 for a $Ni_{81}Fe_{19}$(18 Å)/Au(70 Å)/Co(18 Å) structure, obtained by recording I_{hole} as a function of tip bias at constant hot-electron injection current (I_T=4 nA). The sign of I_{hole} corresponds to holes flowing from the metal stack into the semiconductor back contact. The spectrum labeled *P* (*AP*) is obtained in a magnetic field of +100 Oe (−25 Oe), corresponding to parallel (antiparallel) alignment of the Co and $Ni_{81}Fe_{19}$ magnetizations. The hole current is clearly magnetic field dependent and significantly larger for the parallel magnetic configuration. At the largest applied bias, the current in the *P* state corresponds to a transmission of 0.27 pA per nA of injected current, sufficient to allow magnetic imaging, as shown below.

To exclude artifacts due to possible local variations of the transmission, the hole current was measured while sweeping the magnetic field through a complete cycle from −100 Oe to +100 Oe and back in 0.1 Oe steps. The resulting hole current versus field is shown in the bottom panel of Fig. 2 for constant I_T=4 nA and tip bias V_T=−1.0 V. We observe two field regions (between about ±15 and ±45 Oe) where the hole current is reduced due to *AP* magnetic alignment, a larger current for the *P* state, and the expected magnetic hysteresis. The hole current is 0.36 and 0.13 pA in the *P* and *AP* state, respectively, corresponding to a large magnetocurrent of 180% at V_T=−1.0 V.

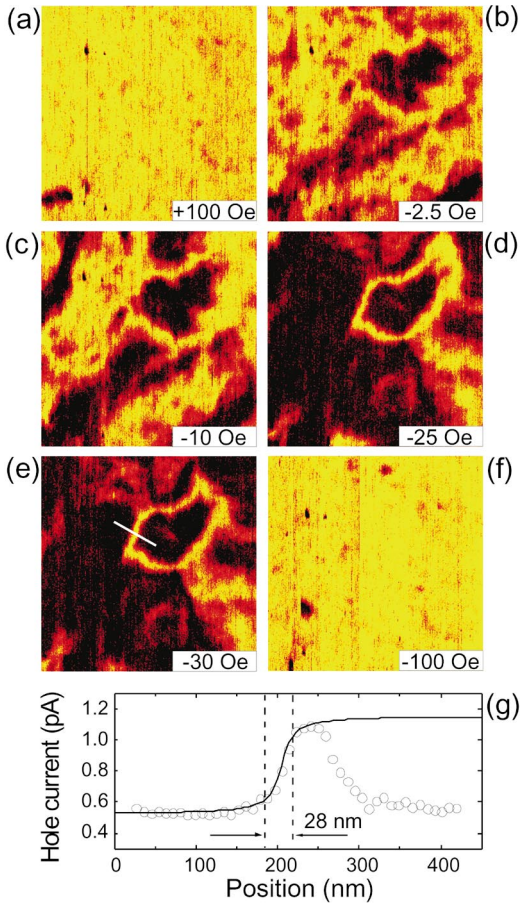

FIG. 3. (Color) R-BHMM images of the spin-dependent hole current in a 2 μm×2 μm area at subsequent magnetic fields of (a) +100 Oe, (b) −2.5 Oe, (c) −10 Oe, (d) −25 Oe, (e) −30 Oe, and (f) −100 Oe. The sample structure is *p*-Si/Au(70 Å)/$Ni_{81}Fe_{19}$(15 Å)/Au(70 Å)/Co(15 Å)/Au(30 Å). Hole current ranges from 0.5 pA (black) to 1.1 pA (yellow). V_T=−1.6 V, I_T=3 nA. In (g) a cross section is shown taken along the white line marked in (e). T=150 K.

Application of spin-dependent hole transport to high-resolution magnetic imaging is demonstrated using a sample with a $Ni_{81}Fe_{19}$(15 Å)/Au(70 Å)/Co(15 Å) stack. Figure 3 presents spatial maps of the collected hole current obtained by scanning the tip across a 2-μm-square area of the sample at different applied magnetic fields. Data were acquired at a tip bias of V_T=−1.6 V and injection current I_T=3 nA. Image 3(a) corresponds to the saturated parallel configuration taken at +100 Oe, and shows a large hole current of about 1.1 pA (in yellow) in the entire area, except for a small region (in black) near the bottom left. When the magnetic field is subsequently reversed to a small negative value [Fig. 3(b)], contrast appears with regions of large hole current (*P* state, yellow) coexisting with regions of reduced current (black) having a local *AP* magnetic orientation. When the field is further increased [images (c)–(e)], the *AP* regions grow at the expense of parallel regions such that most of the magnetic trilayer is now in the *AP* state with hole current of about 0.55 pA. However, a narrow ring-like structure with a large hole current still persists. This is attributed to a 360° domain wall. Note the sharpening of the top-right part of the

ring structure when going from (d) to (e), and the presence of patches in the images with intermediate current (in red) corresponding neither to a fully parallel state, nor to a completely antiparallel state. Also, while most of the area is in the *AP* state, a small portion of the area near the bottom right corner has already returned to the parallel state in (d) taken at −25 Oe, while this region was in the antiparallel state in images (b) and (c). This indicates that local differences in the switching field are present in the sample. For the last image [Fig. 3(f)] subsequently taken at −100 Oe, most of the sample has reversed to a parallel state. Note that the magnetocurrent is about 100%, which is smaller than that in Fig. 2 because of the larger bias and the thinner ferromagnetic layers for the sample used in Fig. 3.

The magnetic resolution was determined from the signal variation along a line crossing the 360° domain wall. As shown in Fig. 3(g), the signal reaches the full value of the parallel state, and the profile is well described by a simple arctan function for a single bit transition (solid line). Defining the transition width as the distance between the points where 20% and 80% of the maximum signal are reached, the width is determined to be 28 nm. Clearly, this value presents an upper limit to the true magnetic resolution, which is probably smaller than 28 nm. Test samples with sharper transitions are needed to examine whether the magnetic resolution can be as small as the 1.5 nm observed using holes on nonmagnetic structures.[6]

In conclusion, we have introduced a technique to investigate magnetic nanostructures and nanoscale spin-transport based on spin dependent transmission of holes from a ferromagnetic stack into a *p*-type semiconductor. Large magnetocurrent up to 180% was observed, and the technique was used to obtain local hysteresis loops and applied to magnetic imaging with resolution below 30 nm.

The authors acknowledge financial support from the Dutch Foundation for Fundamental Research on Matter (FOM), the Royal Netherlands Academy of Arts and Sciences (KNAW), and the European Commission (SPINOSA).

[1]W. J. Kaiser and L. D. Bell, Phys. Rev. Lett. **60**, 1406 (1988).
[2]L. D. Bell and W. J. Kaiser, Annu. Rev. Mater. Sci. **26**, 189 (1996).
[3]M. Prietsch, Phys. Rep. **253**, 163 (1995).
[4]R. Ludeke, A. Bauer, and E. Cartier, Appl. Phys. Lett. **66**, 730 (1995).
[5]W. H. Rippard, A. C. Perrella, and R. A. Buhrman, Appl. Phys. Lett. **78**, 1601 (2001).
[6]T. Meyer and H. von Känel, Phys. Rev. Lett. **78**, 3133 (1997).
[7]W. H. Rippard and R. A. Buhrman, Appl. Phys. Lett. **75**, 1001 (1999).
[8]W. H. Rippard, A. C. Perrella, P. Chalsani, F. J. Albert, J. A. Katine, and R. A. Buhrman, Appl. Phys. Lett. **77**, 1357 (2000).
[9]M. H. Hecht, L. D. Bell, W. J. Kaiser, and L. C. Davis, Phys. Rev. B **42**, 7663 (1990).
[10]L. D. Bell, M. H. Hecht, W. J. Kaiser, and L. C. Davis, Phys. Rev. Lett. **64**, 2679 (1990).
[11]T. Meyer, D. Migas, L. Miglio, and H. von Känel, Phys. Rev. Lett. **85**, 1520 (2000).
[12]A. T. Hanbicki, B. T. Jonker, G. Itskos, G. Kioseoglou, and A. Petrou, Appl. Phys. Lett. **80**, 1240 (2002).
[13]X. Jiang, R. Wang, S. van Dijken, R. Shelby, R. Macfarlane, G. S. Solomon, J. Harris, and S. S. P. Parkin, Phys. Rev. Lett. **90**, 256603 (2003).
[14]T. Banerjee, E. Haq, M. H. Siekman, J. C. Lodder, and R. Jansen, Phys. Rev. Lett. **94**, 027204 (2005).
[15]R. Jansen, J. Phys. D **36**, R289 (2003).
[16]E. Haq, H. Gokcan, T. Banerjee, F. M. Postma, M. H. Siekman, R. Jansen, and J. C. Lodder, J. Appl. Phys. **95**, 6930 (2004).